Evaluation of TiN/Cu Gate Metal Scheme for AlGaN/GaN High-Electron-Mobility Transistor Application

2013 Appl. Phys. Express 6 091003

(http://iopscience.iop.org/1882-0786/6/9/091003)

Applied Physics Express **6** (2013) 091003
http://dx.doi.org/**10.7567/APEX.6.091003**

Evaluation of TiN/Cu Gate Metal Scheme for AlGaN/GaN High-Electron-Mobility Transistor Application

Yueh-Chin Lin[1], Chih-Hsiang Chang[2], Fang-Ming Li[1], Li-Han Hsu[1], and Edward Yi Chang[1,2*]

[1]*Institute of Materials Science and Engineering, National Chiao-Tung University, Hsinchu 30010, Taiwan, R.O.C.*
[2]*Department of Electronics Engineering, National Chiao-Tung University, Hsinchu 30010, Taiwan, R.O.C.*
E-mail: edc@mail.nctu.edu.tw

Received June 26, 2013; accepted August 19, 2013; published online September 9, 2013

The TiN/Cu metal scheme as gate metal for AlGaN/GaN high-electron-mobility transistors (HEMTs) is investigated. The copper-gated devices show comparable DC characteristics to the conventional Ni/Au-gated devices. No obvious of changes in I_{DS} and I_{GS} were observed for the device after being stressed at V_{DS} = 200 and V_{GS} = −5 V for 32 h. The thermal stability test indicates comparable Schottky barrier height for the TiN/Cu gate metal on GaN before and after 250 °C annealing for 1 h. Overall, the AlGaN/GaN HEMT with the TiN/Cu gate metal structure demonstrates excellent device DC characteristics, good thermal stability, and stable performance after a high-voltage stress test.

Recently, wide-bandgap AlGaN/GaN high-electron-mobility transistors (HEMTs) have been widely studied for high-frequency and high-power applications[1–5] due to their excellent thermal stability, high breakdown field, and high saturation drift velocity. In the conventional HEMT process, gold (Au) is usually used as the metallization metal. However, the price of Au is becoming higher and higher; therefore, it is necessary to find a new metallization system without Au to reduce the production cost of AlGaN/GaN HEMT devices. Copper (Cu) metallization has been widely studied since IBM first announced its success in Cu metallization of silicon integrated circuits.[6,7] This is because copper has good electrical conductivity,[8–10] high melting point, high thermal stability, good adhesion to dielectrics, and lower cost.[11,12] Cu is also a good candidate to replace gold as the metallization metal for III–V-based devices; papers on Cu-metallized Ohmic contacts to InGaAs by using Pd/Ge/Cu,[13] Ti/Pt/Ti/Cu-metallized interconnects for AlGaN/GaN HEMTs,[12] and Cu Schottky contact on AlGaN/GaN HEMT[14] have been published in recent years.

The requirements for a good Schottky contact on HEMT devices include high Schottky barrier height, low leakage current, and good thermal stability. Generally, Ni/Au Schottky metal is used for the AlGaN/GaN HEMTs. To use Cu as the Schottky metal, a diffusion barrier material is required, because copper diffuses fast into the semiconductor if there is no diffusion barrier, and this would result in poor Schottky junction, low power handling capability, and increased interface traps.[14] TiN material is a very attractive gate material because of its thermal stability,[15] low resistivity, and high process compatibility.[16] These properties make TiN a good choice as a gate metal for AlGaN/GaN HEMT devices. In this study, the TiN/Cu gate metal structure is used to replace Ni/Au as the gate metal for the AlGaN/GaN HEMTs. The DC characteristics, high-voltage stress characteristics, and thermal stability of the TiN/Cu gate metal structure on AlGaN/GaN HEMTs are investigated in this work.

The TiN/Cu-gated AlGaN/GaN HEMT fabrication process can be divided into the following steps: mesa isolation, Ohmic contact formation, and gate formation. The mesa isolation was the first step and was formed by Cl2 etching using inductively coupled plasma (ICP) with an etching depth of 200 nm to define the active regions. The Ti/Al/Ni/Au multilayer metal was deposited as Ohmic metal and was annealed using a rapid thermal annealing (RTA) system at 800 °C for 60 s in N_2 ambient. The contact resistance of $2.1 \times 10^{-6}\ \Omega\,cm^2$ was achieved as determined by the transfer line method (TLM). Then, the TiN/Cu gate metal was deposited by reactive sputtering. The titanium metallic target was used with 200 watt DC power under N2/Ar atmosphere for TiN deposition. The gate length used was 2 μm. A conventional AlGaN/GaN HEMT with Ti/Al/Ni/Au Ohmic and Ni/Au gate was also fabricated using the same epitaxial wafer for device performance comparison.

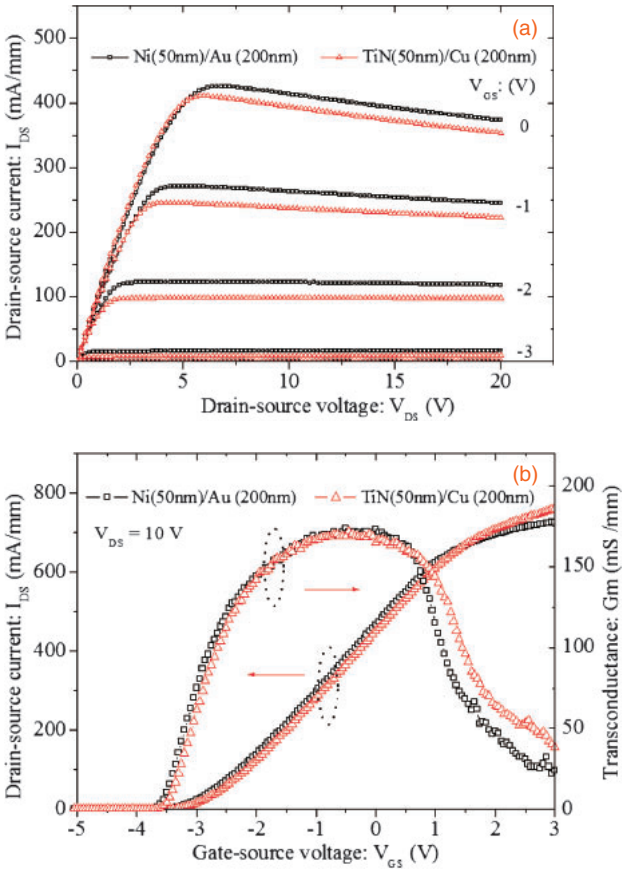

Fig. 1. Comparison of DC characteristics for TiN (50 nm)/Cu (200 nm)- and Ni (50 nm)/Au (200 nm)-gated AlGaN/GaN HEMTs: (a) I_{DS} versus V_{DS} curves, and (b) G_m and I_{DS} versus V_{GS} curves.

Figure 1 shows the comparison of the DC characteristics of the AlGaN/GaN HEMTs with TiN (50 nm)/Cu (200 nm) and the Ni (50 nm)/Au (200 nm) gate structures. When

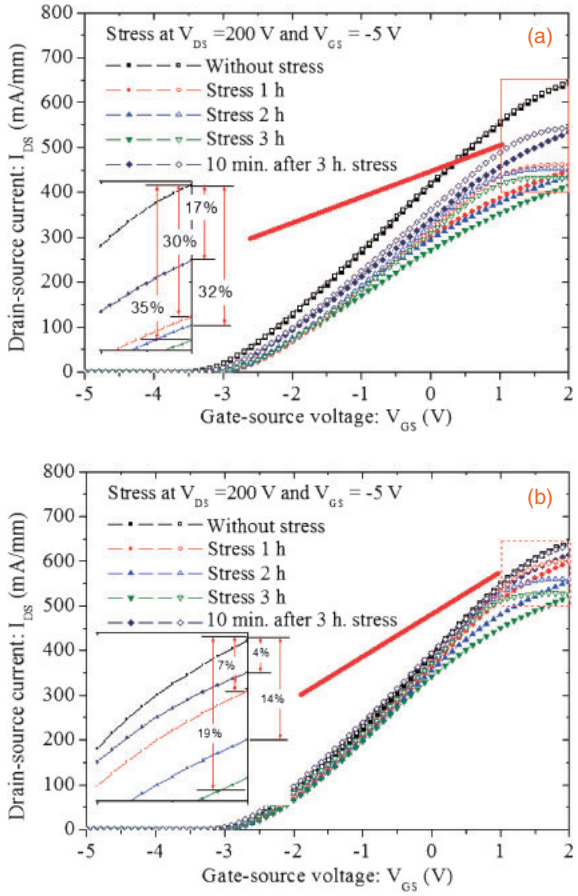

Fig. 2. DC characteristics of HEMTs before high-voltage stress, after high-voltage stress, and 10 min after the high-voltage stress was terminated: (a) I_{DS} versus V_{GS} curves for the Ni (50 nm)/Au (200 nm)-gated AlGaN/GaN HEMTs, and (b) I_{DS} versus V_{GS} curves for TiN (50 nm)/Cu (200 nm)-gated AlGaN/GaN HEMTs.

compared with the Ni/Au-gated device, comparable DC characteristics were obtained for the TiN/Cu-gated device. However, a higher maximum drain–source current ($I_{DS,max}$) at gate–source voltage (V_{GS}) = 3 V was obtained for the TiN/Cu-gated device due to the higher Schottky barrier height of TiN on GaN. The OFF-state breakdown voltage for the Ni/Au and TiN/Cu gate devices were 325 and 346 V, respectively. For the high-voltage stress test, the AlGaN/GaN HEMTs were stressed at a drain–source voltage (V_{DS}) of 200 V with $V_{GS} = -5$ V for different periods of time. The DC characteristics before and after stress for the TiN/Cu-gated and Ni/Au-gated AlGaN/GaN HEMT devices with source–drain spacing of 20 μm and gate–drain distance of 15 μm are shown in Fig. 2, and the V_{GS} bias was setting from −5 to 2 V first and then from 2 to −5 V. It was found that the drain-to-source current (I_{DS}) decreased for both devices after being stressed for 3 h. The current degradation mechanism is believed to be due to the electrically induced defect formation and charge injection when the devices are under high-voltage stress. A large electric field appears under the gate edge across the barrier when the AlGaN/GaN HEMT is under high-voltage operation; this will cause a very large mechanical stress concentrated in a very small region, and the electrically active defects are generated in the AlGaN barrier layer or at its surface in the vicinity of the gate edge, resulting in I_{DS} degradation.[17] Furthermore, the electrons injected from the gate electrode during the high-voltage stress flow into the gate-to-drain region and are captured by the surface states at this region, thus, effectively biasing the surface toward the negative direction. The two-dimensional electron gas (2DEG) density decreased due to the charge neutrality process, which leads to the increase of the drain resistance.[18]

Furthermore, the I_{DS} reduced to 70 and 93% of initial values after being stressed for 1 h for the Ni/Au- and TiN/Cu-gated AlGaN/GaN HEMTs, respectively, as shown in Figs. 2(a) and 2(b). The smaller current degradation for the TiN/Cu-gated HEMT indicates that TiN is more stable than Ni on AlGaN, and fewer electrical defects were produced for the TiN/Cu-gated HEMTs than for the Ni/Au-gated HEMTs. This may be caused by the fact that it is easier for Ni to react with AlGaN when the device was under high-voltage stress. Furthermore, a counter clockwise hysteresis was observed and the hysteresis increased with stress time due to charge injection and the number of electrically active defects on the gate edge of the AlGaN surface increased during the stress test. The direction of the hysteresis suggests that the charges responsible for the collapse came not from the channel but from the gate electrode, which is similar to the operation of floating gate memories.[19] A smaller hysteresis was observed for the TiN/Cu-gated HEMTs due to the higher Schottky barrier height as compared with Ni/Au, which restrained the charge injection during the stress test. The injection charges were released after the stress was stopped; hence, the hysteresis was reduced and I_{DS} was increased just a few minutes after the stress was stopped. However, a small hysteresis of the I_{DS} versus V_{GS} curves remained after the stress was stopped. The I_{DS} degradations were 35 and 19% after 3 h of stress for the Ni/Au-gated and TiN/Cu-gated HEMTs, respectively, and were recovered to 17 and 4% after the stress was stopped for 10 min, indicating that most charge injection was released. Less I_{DS} degradation for TiN/Cu-gated HEMTs than for Ni/Au-gated HEMTs was observed, indicating that TiN did not react as much with AlGaN as Ni when the devices were stressed.

Figure 3 shows the off-state I_{DS} and gate–source current (I_{GS}), and on-state I_{DS} for the TiN/Cu-gated GaN HEMT after a 200 V high-voltage stress test for 32 h. The on-state I_{DS} reduced from 400 to 372 mA/mm due to the increase of surface states and electrical defects during stress, and no obvious changes for the off-state I_{DS} and I_{GS} were found for the TiN/Cu-gated AlGaN/GaN HEMTs. However, the Ni/Au-gated HEMTs shows rapid on-state I_{DS} degradation, and the device failed after high voltage stress test for 10 h. The small current change indicates that the TiN/Cu-gate metal structure was quite stable under high voltage and prolonged stress. For the thermal stability test, the TiN/Cu-gated AlGaN/GaN HEMT devices were annealed at 250 °C for 1 h, and no obvious DC characteristic change was observed after annealing. Furthermore, the I_{DS} decreased to 91% of the initial value after the device was stressed for 1 h as shown in Fig. 4. However, the Ni/Au-gated HEMTs with 250 °C annealing for 1 h failed after high-voltage stress test for just a few min. Compared with the TiN/Cu-gated AlGaN/GaN HEMTs without annealing, no clear current degradation was observed for the annealed device after stressed for 1 h as shown in Fig. 2(b), indicating that the

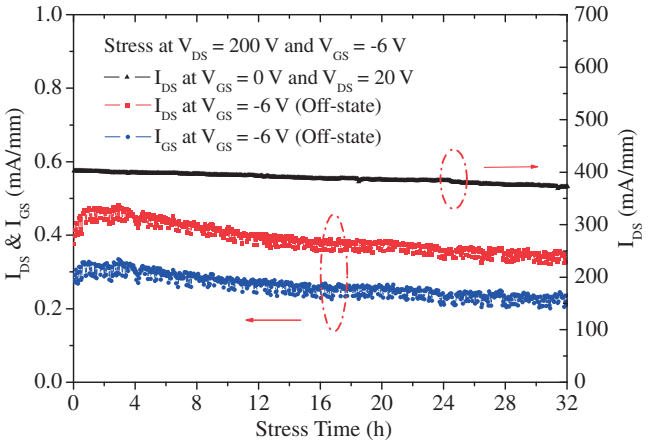

Fig. 3. Off-state drain–source current, off-state gate–source current, and on-state drain–source current for the TiN (50 nm)/Cu (200 nm)-gated AlGaN/GaN HEMT after stress test for 32 h.

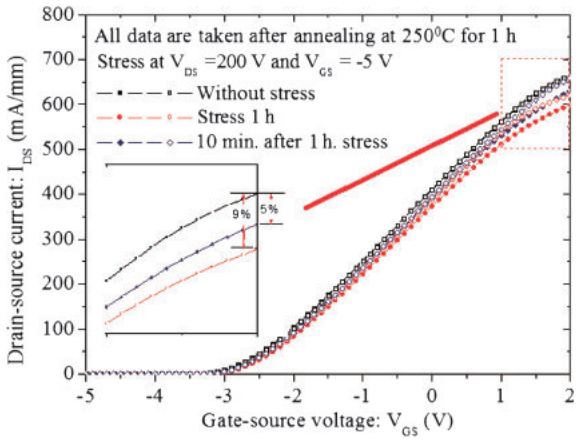

Fig. 4. I_{DS} versus V_{GS} curves for TiN (50 nm)/Cu (200 nm)-gated AlGaN/GaN HEMTs annealed at 250 °C for 1 h for device without high-voltage stress, with high-voltage stress and 10 min after the high-voltage stress was terminated.

TiN/Cu gate structure has excellent thermal stability. Figure 5 shows the forward current–voltage characteristics and Schottky barrier heights with different annealing temperatures. No obvious change in the Schottky barrier height was observed. The Schottky barrier height[20] of the Ti/Cu gate metal on AlGaN was 0.67 eV before annealing and 0.65 eV after thermal annealing at 250 °C for 1 h. (Schottky barrier height for Ni/Au = 0.62 eV.) The Ti/Cu gate metal on AlGaN/GaN HEMT demonstrates good Schottky barrier height with excellent thermal stability.

In summary, TiN/Cu-gated AlGaN/GaN HEMTs were successfully fabricated. The devices show electrical performance comparable to the conventional Ni/Au-gated devices. No obvious changes in I_{DS} and I_{GS} were observed for the device after being stressed at $V_{DS} = 200$ V and $V_{GS} = -5$ V for 32 h. Thermal stability test indicates stable Schottky barrier height for the TiN/Cu gate metal on GaN before and after 250 °C annealing for 1 h. The results indicate that the TiN/Cu gate metal structure can be used for AlGaN/GaN HEMTs with excellent electrical characteristics, good thermal stability, and device reliability.

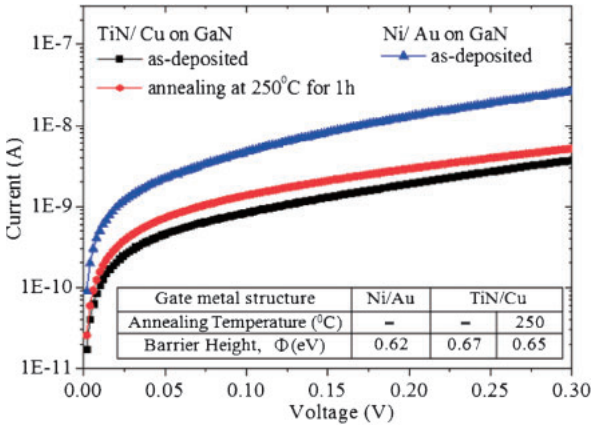

Fig. 5. Forward current–voltage characteristics and Schottky barrier height with different annealing temperatures for the TiN (50 nm)/Cu (200 nm) on GaN Schottky diode (area: 1.96×10^{-5} cm^2).

Acknowledgment The authors would like to thank the National Science Council of the Republic of China for supporting this research under contracts 102-2911-I-009-302- and 101-2221-E-009-173-MY2.

1) Z. Fan, S. N. Mohammad, Ö. Aktas, A. E. Botchkarev, A. Salvador, and H. Morkoç: Appl. Phys. Lett. **69** (1996) 1229.
2) T. Fujii, N. Tsuyukuchi, M. Iwaya, S. Kamiyama, H. Amano, and I. Akasaki: Jpn. J. Appl. Phys. **45** (2006) L1048.
3) F. Stengel, S. N. Mohammad, and H. Morkoç: J. Appl. Phys. **80** (1996) 3031.
4) H. Morkoç, S. Strite, G. B. Gao, M. E. Lin, B. Sverdlov, and M. Burns: J. Appl. Phys. **76** (1994) 1363.
5) U. K. Mishra, P. Parikh, and Y.-F. Wu: Proc. IEEE **90** (2002) 1022.
6) K. Holloway, P. M. Fryer, C. Cabral, Jr., J. M. E. Harper, P. J. Bailey, and K. H. Kelleher: J. Appl. Phys. **71** (1992) 5433.
7) D.-S. Yoon, H. K. Baik, and S.-M. Lee: J. Appl. Phys. **83** (1998) 8074.
8) C. H. Lin, J. P. Chu, T. Mahalingam, T. N. Lin, and S. F. Wang: J. Electron. Mater. **32** (2003) 1235.
9) C.-Y. Chen, C. Li, L. Chang, and S.-H. Chen: IEEE Trans. Electron Devices **48** (2001) 1033.
10) S.-W. Chang, S.-W. Chang, C.-S. Lee, K.-S. Chen, C.-W. Tseng, and T.-L. Hsieh: IEEE Trans. Electron Devices **51** (2004) 1053.
11) Y. C. Wu, E. Y. Chang, Y. C. Lin, H. T. Hsu, S. H. Chen, W. C. Wu, L. H. Chu, and C. Y. Chang: IEEE Microwave Wireless Components Lett. **17** (2007) 133.
12) Y.-C. Lin, T.-Y. Kuo, Y.-L. Chuang, C.-H. Wu, C.-H. Chang, K.-N. Huang, and E. Y. Chang: Appl. Phys. Express **5** (2012) 066503.
13) Y. C. Lin, S.-L. Shie, T.-E. Shie, Y.-Y. Wong, K. S. Chen, and E. Y. Chang: J. Electron. Mater. **40** (2011) 289.
14) M. Esposto, V. D. Lecce, M. Bonaiuti, and A. Chini: J. Electron. Mater. **42** (2013) 15.
15) Y. X. Liu, S. Kijima, E. Sugimata, M. Masahara, K. Endo, T. Matsukawa, K. Ishii, K. Sakamoto, T. Sekigawa, H. Yamauchi, Y. Takanashi, and E. Suzuki: IEEE Trans. Nanotechnol. **5** (2006) 723.
16) J. Widiez, M. Vinet, T. Poiroux, P. Holliger, B. Previtali, P. Grosgeorges, M. Mouis, and S. Deleonibus: IEEE Int. SOI Conf., 2005, p. 30.
17) J. A. del Alamo and J. Joh: Microelectron. Reliab. **49** (2009) 1200.
18) J. A. Mittereder, S. C. Binari, P. B. Klein, J. A. Roussos, D. S. Katzer, D. F. Storm, D. D. Koleske, A. E. Wickenden, and R. L. Henry: Appl. Phys. Lett. **83** (2003) 1650.
19) T. Mizutani, Y. Ohno, M. Akita, S. Kishimoto, and K. Maezawa: IEEE Trans. Electron Devices **50** (2003) 2015.
20) G. Cankaya and N. Ucar: J. Physiol. Sci. **59** (2004) 795.